

Inhibitors of the C_2 -Symmetric HIV-1 Protease: Nonsymmetric Binding of a Symmetric Cyclic Sulfamide with Ketoxime Groups in the P2/P2' Side Chains

Johan Hultén,[†] Hans O. Andersson,[‡] Wesley Schaal,[†] Helena U. Danielson,[§] Björn Classon,[∇] Ingemar Kvarnström,[⊥] Anders Karlén,[†] Torsten Unge,[‡] Bertil Samuelsson,^{||} and Anders Hallberg*,[†]

Department of Organic Pharmaceutical Chemistry, Uppsala Biomedical Centre, Uppsala University, Box 574, SE-751 23 Uppsala, Sweden, Department of Cell and Molecular Biology, Uppsala Biomedical Centre, Uppsala University, Box 596, SE-751 24 Uppsala, Sweden, Department of Biochemistry, Uppsala Biomedical Centre, Uppsala University, Box 576, SE-751 23 Uppsala, Sweden, Medivir AB, Lunastigen 7, SE-141 44 Huddinge, Sweden, Department of Chemistry, Linköping University, SE-581 83 Linköping, Sweden, and Department of Organic Chemistry, Arrhenius Laboratory, Stockholm University, SE-106 91 Stockholm, Sweden

Received April 8, 1999

Symmetric cyclic sulfamides, substituted in the P2/P2' position with functional groups foreseen to bind preferentially to the S2/S2' subsites of HIV-1 protease, have been prepared. Despite efforts to promote a symmetric binding, the sulfamides seemed prone to bind nonsymmetrically, as deduced from X-ray crystal structure analysis of one of the most potent inhibitors, possessing ketoxime groups in the P2/P2' side chains. Ab initio calculations suggested that the nonsymmetric conformation of the cyclic sulfamide scaffold had lower energy than the corresponding symmetric, cyclic urea-like conformation.

Introduction

Inhibition of HIV-1 protease in vitro results in the production of virions that are immature and noninfectious.¹ HIV-1 protease inhibitors, used mainly in combination with reverse transcriptase inhibitors, have been shown to reduce the viral load and increase the number of CD4⁺ lymphocytes in HIV-infected individuals.^{2–5} The clinical emergence of resistant mutants suggests that there will be a need for an ever increasing armament of new drugs that will preferably have a unique pattern of resistance development and good bioavailability.^{6–9}

Today there is a large abundance of structural information on the HIV-1 protease that has been generated by X-ray crystallography^{10–13} and also in recent years by 2D-NMR spectroscopy.^{14–18} A tetrahedrally coordinated structural water (W301)¹⁰ is commonly found in the 3D structures of linear peptidomimetic HIV-1 protease inhibitors. This water is symmetrically positioned and bridges the two flaps of the dimeric enzyme to two carbonyl groups of the inhibitors. Lam et al. took advantage of the structural information obtained from X-ray structures in an elegant design of potent nonpeptidic cyclic urea inhibitors, i.e., DMP323,¹⁹ where the urea oxygen replaces and mimics the bridging structural water.

We prepared the carbohydrate-based, C_2 -symmetric, cyclic urea **1** and the cyclic sulfamide **2** (Figure 1), both containing functionalities that mimic the tetrahedrally coordinated structural water, and compared the X-ray structures of the inhibitor/protease complexes.^{20,21} This comparison revealed an unexpected binding of **2**. The

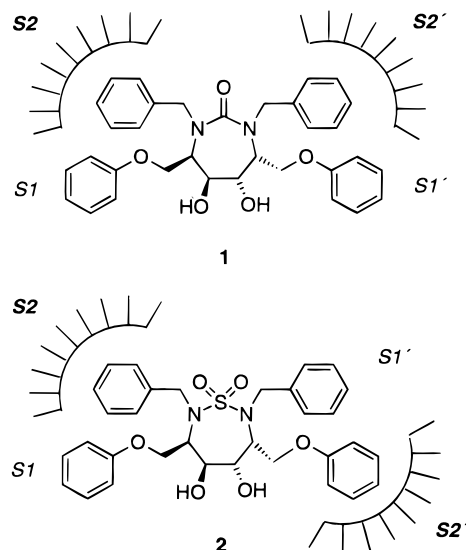


Figure 1. Urea compound **1** with symmetric binding and sulfamide **2** with nonsymmetric binding to the HIV-1 protease.

cyclic sulfamide scaffold adopts a nonsymmetric conformation which places the P2' side chain into the S1' subsite and the P1' side chain into the S2' subsite.²¹ To guide further design prior to the initiation of a more extensive medicinal chemistry program, based on the core structure of **2**, we were prompted to determine whether a symmetric binding of the symmetrically substituted cyclic sulfamides could be induced. After some exploratory modeling, we decided to prepare six cyclic sulfamides, **3–8**, that were symmetrically substituted in the P2/P2' positions with functional groups foreseen to bind preferentially to the S2/S2' subsites.

Results and Discussion

Synthesis. The iodo derivative **11** served as a precursor in the palladium-catalyzed reactions to provide the

* Corresponding author.

[†] Department of Organic Pharmaceutical Chemistry, UBC.

[‡] Department of Cell and Molecular Biology, UBC.

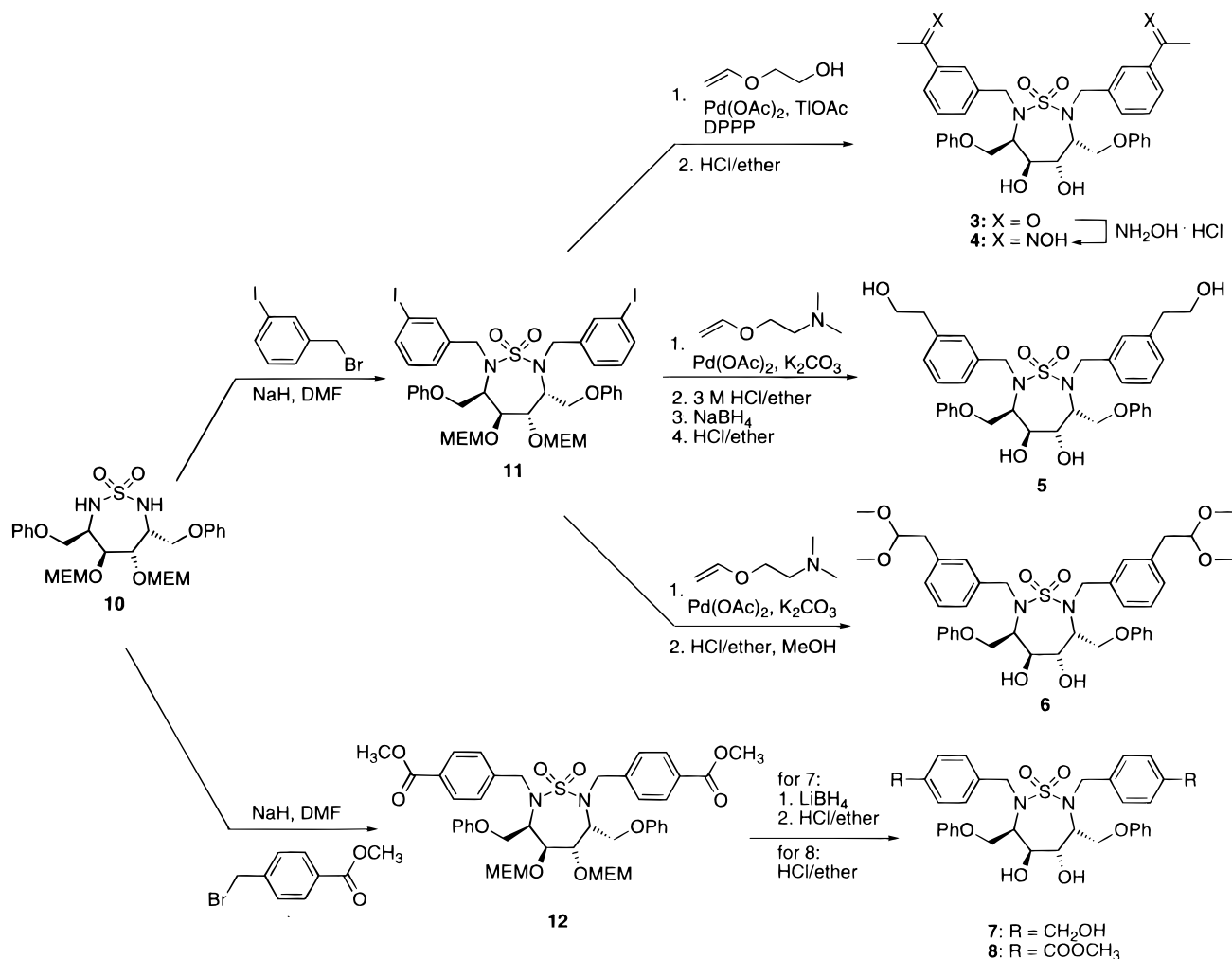
[§] Department of Biochemistry, UBC.

[∇] Medivir AB.

[⊥] Linköping University.

^{||} Stockholm University.

Scheme 1

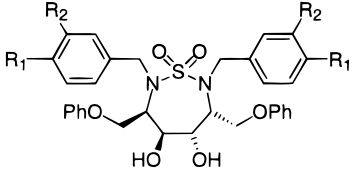


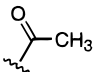
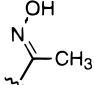
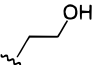
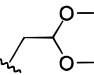
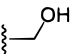
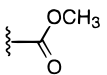
compounds **3–6** (Scheme 1). Compound **11** was obtained in 80% yield after alkylation of the parent sulfamide **10**²⁰ with 3-iodobenzyl bromide in the presence of NaH in DMF. Aryl methyl ketones can be prepared by Heck arylation of alkyl vinyl ethers²² and with very high regioselectivity in the presence of bidentate ligands, as demonstrated by Cabri et al.²³ In our first attempts to prepare **3** from **11** via palladium-catalyzed arylation, where the commonly used butyl vinyl ether was employed as olefin, a moderate yield was encountered. However, the ligand-directed regiocontrolled α -arylation of 2-hydroxyethyl vinyl ether with 1,3-bis(diphenylphosphino)propane (DPPP) as ligand²⁴ provided **3** in 83% yield after subsequent treatment with HCl/ether and methanol. The ketoxime derivative **4** was prepared from **3** by treatment with hydroxylamine hydrochloride in ethanol.²⁵ A Heck arylation designed to promote β -arylation by palladium–nitrogen chelation control²⁶ furnished compounds **5** and **6**. Thus, the selective β -arylation of [2-(dimethylamino)ethoxy]ethene and subsequent hydrolysis in a two-phase system led to deprotection of the vinyl ether and delivered the corresponding aldehyde. Reduction of the intermediate aldehyde with NaBH₄ followed by deprotection of the MEM groups provided the hydroxyethyl derivative **5** in 19% yield over four steps. Treatment of the β -arylated vinyl ether with HCl/ether in methanol yielded the methyl acetal **6**. Compound **12** was obtained in 80% yield from **10** after

alkylation with methyl 4-bromomethylbenzoate in the presence of NaH in DMF. The ester groups of **12** were thereafter smoothly reduced²⁷ with excess LiBH₄ to afford the hydroxymethyl derivative **7** after deprotection. Compound **12** was transformed to **8** in a mixture of HCl/ether and methanol.

HIV Protease Inhibition. The HIV-1 protease was cloned and heterologously expressed in *Escherichia coli* and purified as described elsewhere.²⁸ The K_i values for the synthesized compounds were determined by a fluorometric assay²⁹ (Table 1).

Modeling. To determine whether a sulfamide-based inhibitor could be expected to adopt a urea-like conformation, we performed calculations on the symmetric and nonsymmetric conformation of the models of **2** (Figure 2). Other possible ring conformations were not explored. Ab initio calculations on the two model conformations at the B3LYP/6-31G* level of theory indicated that the nonsymmetric conformation was 2.4 kcal/mol lower in energy than the symmetric conformation. This penalty seemed low enough to be considered surmountable with substituents that anchor the P2/P2' side chains in the S2/S2' subsites through interactions with Asp29, Asp30, and Gly48. For information about the interactions with these possible anchoring points in the S2/S2' subsite, we searched the Protein Data Bank^{30,31} for coordinates for DMP323,³² a urea-based inhibitor with hydroxymethyl substituents in the para

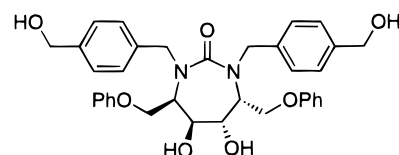
Table 1. Inhibitory Activity of Cyclic Sulfamide Compounds Against HIV-1 Protease


compd	R ₁	R ₂	K _i (nM) ^a
2	H	H	19
3 ^b	H		59
4 ^b	H		3.4
5	H		43
6	H		540
7 ^b		H	3.1
8		H	84

^a K_i values for compounds **3–8** were determined using a spectrofluorometric assay.²⁹ ^b K_i values for related cyclic urea compounds with acetyl (K_i = 0.06 nM), ketoxime (K_i = 0.018 nM), and hydroxymethyl (K_i = 0.27 nM) substituents have been reported by DuPont-Merck.^{19,35}

**Figure 2.** Superimposition of the symmetric (dark gray) and nonsymmetric (light gray) conformation of the cyclic sulfamide scaffold.

positions of the P2/P2' side chains. However, at the time of this investigation the X-ray coordinates for DMP323 in the native enzyme were not available. Therefore, we

Chart 1. Urea Compound **9**

crystallized and analyzed the 3D structure of the carbohydrate-derived cyclic urea inhibitor **9** (Chart 1), an analogue to DMP323 that had been previously prepared. As expected, the inhibitor binds in a symmetric conformation and the hydroxymethyl substituents are interacting with the backbone amide NH of Asp30/30'. Furthermore, well-ordered water molecules tight packing to the aromatic rings of the P1/P2 and P1'/P2' side chains are seen distinctly.

Models for both the symmetric (urea-like) and non-symmetric (flipped) conformations of **3–8** were made to help anticipate their potential interactions in the HIV-1 protease binding site. The modeling of compound **4** was complicated by the fact that the *E/Z* configuration of the ketoximes was not easily predictable. A search of the Cambridge Structural Database³³ for acetophenone oximes revealed that the *E* configuration was more frequent than the *Z* configuration.³⁴

In the models of the symmetric conformations, P2 and P2' were directed into the S2 and S2' pockets. The R₁ and R₂ functional groups (see Table 1) were generally seen to participate in hydrogen bonding to Asp29/29' and/or Asp30/30'. The carbonyl oxygens of **3** and **8** and also the hydroxyl oxygens of **4** and **7** could form hydrogen bonds with the backbone NH of either Asp29/29' or Asp30/30'. Furthermore the hydroxyl group of **4**, **5** and **7** could form hydrogen bonds to the carboxylate side chain of either Asp29/29' or Asp30/30'. The acetal of **6** and the ester group of **8** were directed toward the solvent.

In the models of the nonsymmetric conformations, P2 and P2' were directed into the S2 and S1' pockets, respectively. Interactions in the S2 pockets generally followed the pattern seen for the symmetric conformations. Interactions in the S1' pockets focused around Arg8. The P2 carbonyl group of **3** and **8** and the acetal group of **6** were directed primarily into the solvent. The P2 hydroxyl groups of **4** and **5** could form hydrogen bonds to the carboxylate side chain of Asp30. The P2 hydroxyl group of **7** could form a hydrogen bond to the carbonyl backbone of Asp30. The P2' carbonyl oxygen of **3** and **8**, the acetal of **6**, and the hydroxyl groups of **4**, **5**, and **7** could form hydrogen bonds with the guanidino group of Arg8. In conclusion, the modeling study predicts that fewer hydrogen bond interactions are available in the S1' pocket.

Biological Results. The K_i values of **3–8** are shown in Table 1. The inhibitor **4**, substituted with two ketoxime functions, exhibited a K_i value of 3.4 nM as compared to 19 nM for the parent compound **2**. Oxime functionalities when applied to the cyclic urea series were recently found to furnish inhibitors with very high potency, and a methyl ketoxime related to **4** had a K_i of 0.018 nM.³⁵ Han and Lam reported that each of the hydroxyl groups of the ketoxime in the urea derivative donates a hydrogen bond to the carboxylate side chain of Asp30/30', located in the S2/S2' subsite. Furthermore,

each nitrogen of the ketoxime groups accepts a hydrogen bond from the backbone amide NH of Asp30/30' as deduced from the X-ray crystal structures. The hydroxymethyl-substituted sulfamide inhibitor **7**, which exhibited an almost identical K_i (3.1 nM) as compared to the ketoxime **4**, is 10-fold less potent than the corresponding urea analogue **9**. Compound **5** was a poor inhibitor despite modeling suggesting that the hydroxyethyl substituents could interact with Asp30/30'. Compounds **3** and **8** with hydrogen bond-accepting keto and ester carbonyl groups were both weak inhibitors of the protease and exhibited K_i values of 59 and 84 nM, respectively. The acetal derivative **6**, anticipated from modeling experiments to allow for a favorable interaction with Arg8, was in fact the worst inhibitor in the series and found to be 20-fold less potent than the parent sulfamide **2**.

On the basis of the difference in K_i values between the sulfamides **3**, **4**, **7** and the corresponding ureas, we anticipate that the cyclic sulfamides were all binding in an nonsymmetric conformation to the enzyme. The difference in desolvation energy for urea and sulfamide could account for part of this difference in affinity. However, previous molecular dynamic calculations showed no indication of different desolvation energy for **2** as compared to **1**.²⁰ We were encouraged to obtain a 3D structure of one of the sulfamide compounds to elucidate this issue. Ultimately we were successful in obtaining good crystals of the HIV protease complex with one of the most potent inhibitors of the series, the ketoxime **4** (Figure 3), and the 3D structure was determined to 1.80 Å resolution with a R_{cryst} of 21.2% ($R_{\text{free}} = 23.6\%$). The analysis of the data established that **4**, designed with P2/P2' substituents anticipated to strongly bind to the S2/S2' subsites, in fact, adopted a nonsymmetrical binding mode with the P2' aryl ketoxime substituent positioned in the S1' subsite (Figure 4). The ketoxime group located in the S2 subsite has the *E* configuration around the double bond which results in a hydrogen bond between the hydroxyl group of the ketoxime and the carboxylate side chain of Asp30. Han and Lam reported a corresponding hydrogen bond in the cyclic urea ketoxime and in addition to this a hydrogen bond between the nitrogen of the ketoxime and the backbone amide NH of Asp30. The latter interaction is however not present in the complex between the sulfamide ketoxime **4** and the protease. Structural water molecules with interactions similar to the water molecules found in the complex of inhibitor **9** and the protease are also observed. The electron density for the ketoxime group in the S1' subsites is missing, indicating that the ketoxime lacks specific interactions with the protease or structural water molecules. Considering the P2' aryl ketoxime substituent in the lipophilic S1' subsite, a displacement of the structural water seemed feasible. However, such displacement of the structural water did not take place as deduced from the X-ray structure (see Figure 3).³⁶ Thus only one of the ketoxime groups seems to interact favorably with the protease. This leads to fewer interactions of inhibitor **4**, as compared to the urea analogue, and could provide part of the explanation for the lower activity of the sulfamide analogue. The 10-fold lower activity of compound **7** as compared to **9** can also be explained if it is

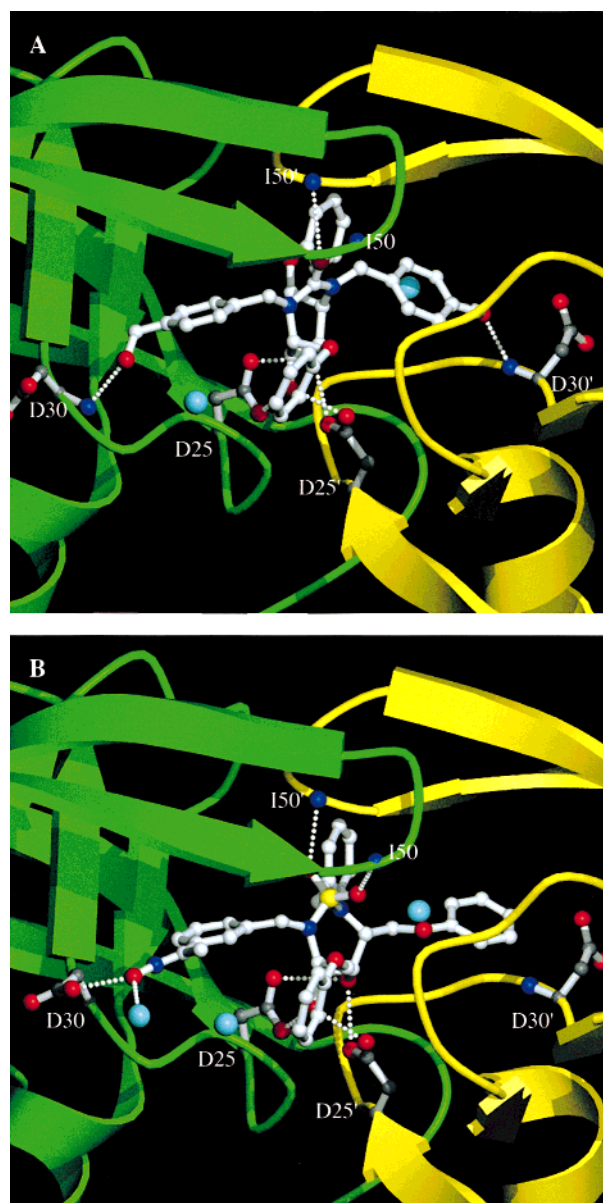


Figure 3. Conformation of compounds **9** (panel A) and **4** (panel B) in the HIV-1 protease active site (chain A colored green and chain B yellow). (A) Inhibitor **9**, with a K_i of 0.23 nM, adopts a symmetric conformation. Consequently, the P1/P2 and P1'/P2' side chains have identical interactions with the corresponding subsites. The hydroxymethyl substituents are interacting with the backbone amide NH of Asp30/30'. (B) Compound **4** binds in a nonsymmetric conformation: i.e., the P2 side chain is located in the S2 subsite, whereas the P2' side chain is in the S1' subsite. In the S2 subsite, hydrogen bonds are formed between the hydroxyl group of the ketoxime and the carboxylate side chain of Asp30 (2.9 Å) and a water molecule (2.7 Å). In the S1 subsite there are no suitable interactions for the ketoxime group. No electron density was detected for the P2' ketoxime group in the $2F_{\text{obs}} - F_{\text{calc}}$ map. Conserved water molecules (light blue) are located between the P1/P2 and P1'/P2' side chains in both complexes. The figure was drawn with the program MOLSCRIPT 2.02.⁵⁰

assumed that only one of the hydroxymethyl substituents in **7** is interacting favorably with the S2/S2' subsite.¹¹

Conclusion

In summary, our results suggest that the cyclic sulfamide core structure is not prone to adopt a cyclic

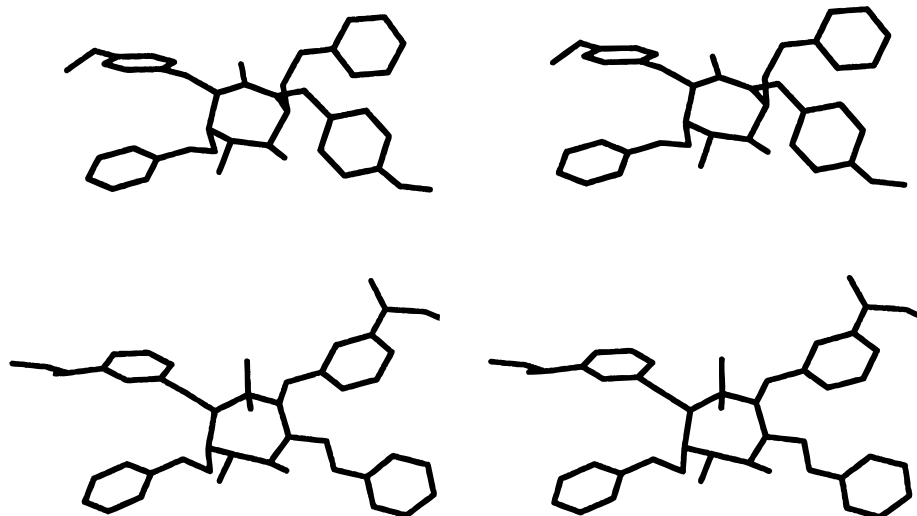


Figure 4. Stereoview of the X-ray structure of inhibitor **9** (top) and inhibitor **4** (bottom), showing the conformation of the cyclic sulfamide scaffold and the direction of the P2/P2' and P1/P1' side chains. The position of the P2' ketoxime of **4** was determined by modeling.

urea conformation and consequently that the structure–activity relationship for the two classes of compounds should differ considerably. On the basis of ab initio calculations of a truncated form of the cyclic sulfamides, the nonsymmetric conformation was found to be 2.4 kcal/mol lower in energy than the symmetric urea-like form. This penalty seemed low enough to be considered surmountable with substituents that anchor the P2/P2' side chains in the S2/S2' subsites. However, the X-ray crystal structure of inhibitor **4** clearly shows a nonsymmetric mode of binding despite efforts to induce a symmetric binding through symmetrically substituted ketoxime groups in P2/P2' side chains.

Experimental Section

Chemistry. General Information. Melting points were recorded on an Electrothermal melting point apparatus and are uncorrected. Optical rotations were obtained on a Perkin-Elmer 241 polarimeter. Specific rotations ($[\alpha]_D$) are reported in degrees/decimeter and the concentration (c) is given in grams/100 mL in the specific solvent. ^1H and ^{13}C NMR spectra were recorded on a JEOL JNM-EX 270 spectrometer at 270.2 and 67.8 MHz, respectively, or on a JEOL JNM-EX 400 spectrometer at 399.8 and 100.5 MHz, respectively, and the chemical shifts are given in ppm relative to tetramethylsilane. Infrared spectra were recorded on a Perkin-Elmer 1600 series FTIR instrument. Elemental analyses were performed by MikroKemi AB, Sweden, or Analytische Laboratorien, Germany, and were within $\pm 0.4\%$ of calculated values. Mass spectroscopy was carried out on a JEOL SX 102 instrument. Flash column chromatography was performed on silica gel 60, 0.04–0.063 mm (E. Merck), with gradient elution unless otherwise noted. Thin-layer chromatography was performed on precoated silica gel F-254 plates (0.25 mm; E. Merck) and was visualized with UV light and H_2SO_4 in ethanol or phosphomolybdic acid or ninhydrin. Standard workup: organic layers were dried with MgSO_4 and concentrated in vacuo.

(3R,4S,5S,6R)-2,7-Bis[(3-acetylphenyl)methyl]-4,5-dihydroxy-3,6-bis(phenoxyethyl)-1,2,7-thiadiazepine 1,1-Dioxide (3). Into the reaction vessel were added $\text{Pd}(\text{OAc})_2$ (0.81 mg, 0.0036 mmol), DPPP (2.97 mg, 0.0072 mmol), and a small amount of DMF (1.0 mL). To this mixture were added Et_3N (18.3 mg, 0.18 mmol) and compound **11** (50 mg, 0.050 mmol) followed by addition of TIOAc (37.9 mg, 0.144 mmol), 2-hydroxyethyl vinyl ether (58.3 mg, 0.66 mmol), and DMF (1.0 mL). The reaction mixture was heated at 80 °C overnight. After cooling, the reaction mixture was partitioned between

water and diethyl ether. The solvent was removed and to the crude product in methanol (5 mL) was added wet HCl in ether (10 mL). The reaction mixture was stirred overnight at 25 °C. The solvent was removed and purification by flash column chromatography on silica ($\text{CH}_2\text{Cl}_2/\text{CH}_3\text{OH}$, 200:1) gave the product as an oil (27 mg, 82%): IR (CHCl_3) ν 1682, 1598, 1496, 1437 cm^{-1} ; $[\alpha]_D = +15.8^\circ$ ($c = 0.36$, CHCl_3 , 22 °C); ^1H NMR (270.2 MHz, CDCl_3) δ 7.92 (s, 2H), 7.75 (d, $J = 7.7$ Hz, 2H), 7.68 (d, $J = 7.7$ Hz, 2H), 7.36 (t, $J = 7.7$ Hz, 2H), 7.16 (appt, $J = 7.8$ Hz, 4H), 6.89 (t, $J = 7.2$ Hz, 2H), 6.63 (d, $J = 8.4$ Hz, 4H), 4.90 (m, 4H), 4.32 (m, 4H), 4.17 (dd, $J = 9.6$, 5.1 Hz, 2H), 4.08 (dd, $J = 9.7$, 6.1 Hz, 2H), 3.39 (brs, 2H), 2.47 (s, 6H); ^{13}C NMR (100.2 MHz, CDCl_3) δ 198.3, 157.5, 139.0, 137.2, 132.4, 129.6, 129.0, 127.6, 127.3, 121.7, 114.4, 75.1, 67.1, 55.6, 52.9, 26.7. Anal. ($\text{C}_{36}\text{H}_{38}\text{N}_2\text{O}_8\text{S}\cdot 0.5\text{H}_2\text{O}$) C, H, N.

(3R,4S,5S,6R)-2,7-Bis[(3-methoxyimophenyl)methyl]-4,5-dihydroxy-3,6-bis(phenoxyethyl)-1,2,7-thiadiazepine 1,1-Dioxide (4). To a solution of compound **3** (43 mg, 0.065 mmol) in a mixture of ethanol (2 mL) and water (1 mL) were added hydroxylamine hydrochloride (23 mg, 0.33 mmol) and NaOH (41 mg, 1.0 mmol). The reaction mixture was heated at 60 °C for 3 h. The solvent was removed and purification by flash column chromatography on silica ($\text{CH}_2\text{Cl}_2/\text{CH}_3\text{OH}$, 50:1) gave the product as a white solid (32 mg, 73%): ^1H NMR (399.2 MHz, CD_3OD) δ 7.76 (s, 2H), 7.49 (d, $J = 7.8$ Hz, 2H), 7.46 (d, $J = 7.8$ Hz, 2H), 7.27 (t, $J = 7.8$ Hz, 2H), 7.18 (dd, $J = 8.8$, 7.5 Hz, 4H), 6.87 (t, $J = 7.4$ Hz, 2H), 6.73 (d, $J = 8.8$ Hz, 4H), 5.05 (d, $J = 17.9$ Hz, 2H), 4.92 (d, $J = 17.6$ Hz, 2H), 4.41 (t, $J = 6.7$ Hz, 2H), 4.13 (m, 6H), 2.19 (s, 6H); ^{13}C NMR (67.8 MHz, acetone- d_6) δ 159.1, 154.3, 141.0, 138.1, 130.1, 128.9, 128.2, 125.4, 125.0, 121.6, 115.3, 74.7, 67.1, 55.7, 52.7, 11.5. Anal. ($\text{C}_{36}\text{H}_{40}\text{N}_4\text{O}_8\text{S}\cdot 1.0\text{H}_2\text{O}$) C, H, N.

(3R,4S,5S,6R)-2,7-Bis[(3-(2-hydroxyethyl)phenyl)methyl]-3,6-bis(phenoxyethyl)-4,5-dihydroxy-1,2,7-thiadiazepine 1,1-Dioxide (5). Into the reaction vessel were added K_2CO_3 (21.9 mg, 0.158 mmol), LiCl (11.2 mg, 0.264 mmol), NaOAc (12.99 mg, 0.158 mmol), and DMF (1.0 mL). To this mixture were added $\text{Pd}(\text{OAc})_2$ (2.96 mg, 0.0132 mmol) and compound **11** (55.5 mg, 0.055 mmol) followed by addition of water (0.11 mL) and [2-(dimethylamino)ethoxy]ethene (38.0, 0.329 mmol). The reaction mixture was heated at 80 °C overnight. After cooling, the reaction mixture was partitioned between water and diethyl ether. The solvent was removed, the crude product was dissolved in diethyl ether (15 mL), 3 M HCl aq (15 mL) was added, and the reaction mixture was stirred vigorously overnight at 25 °C. The ether layer was separated and the aqueous layer was extracted with ether (2×20 mL). The combined ether extracts were dried and concentrated in vacuo. The crude aldehyde was dissolved in methanol (3 mL) at 0 °C. To this solution was added NaBH_4

(6.3 mg, 0.167 mmol). The reaction mixture was stirred overnight under N₂ atmosphere, slowly rising the temperature to room temperature, and thereafter HCl in ether (5 mL) was added and stirred overnight at room temperature. The solvent was removed and purification by flash column chromatography on silica (CH₂Cl₂/CH₃OH, 50:1) gave the product as a white solid (12.8 mg, 19%): IR (CHCl₃) ν 3684, 3603, 1597, 1495 cm⁻¹; [α]_D = +5.8° (*c* = 0.72, CHCl₃, 22 °C); ¹H NMR (399.8 MHz, CDCl₃) δ 7.32 (m, 6H), 7.09 (d, *J* = 7.3 Hz, 2H), 6.96 (t, *J* = 7.4 Hz, 2H), 6.72 (d, *J* = 7.8 Hz, 4H), 4.77 (m, 4H), 4.30–4.10 (m, 8H), 3.75 (t, *J* = 6.4 Hz, 4H), 3.31 (brs, 2H), 2.77 (t, *J* = 6.4 Hz, 4H), 1.68 (brs, 2H); ¹³C NMR (100.2 MHz, CDCl₃) δ 157.6, 139.1, 138.2, 129.6, 128.9, 128.5, 128.4, 126.0, 121.6, 114.5, 75.1, 66.7, 63.5, 56.2, 53.0, 39.0. Anal. (C₃₆H₄₂N₂O₈S) C, H, N.

(3R,4S,5S,6R)-2,7-Bis[3-(2,2-dimethoxyethyl)phenyl]methyl-4,5-dihydroxy-3,6-bis(phenoxymethyl)-1,2,7-thiadiazepine 1,1-Dioxide (6). Into the reaction vessel were added K₂CO₃ (21.9 mg, 0.158 mmol), LiCl (11.2 mg, 0.264 mmol), NaOAc (12.99 mg, 0.158 mmol), and DMF (1.0 mL). To this mixture were added Pd(OAc)₂ (2.96 mg, 0.0132 mmol) and compound **11** (55.5 mg, 0.055 mmol) followed by addition of water (0.11 mL) and [2-(dimethylamino)ethoxy]ethane (38.0, 0.329 mmol). The reaction mixture was heated at 80 °C overnight. After cooling, the reaction mixture was partitioned between water and diethyl ether. The solvent was removed, the crude product was dissolved in methanol (5 mL), and saturated HCl in ether (10 mL) was added. The reaction mixture was stirred overnight and concentrated in vacuo. Purification by flash column chromatography on silica gel (CH₂Cl₂, 200:1) gave a colorless oil (18.8 mg, 39%): IR (film) ν 3600–3200, 1701, 1599, 1496 cm⁻¹; ¹H NMR (270.2 MHz, CDCl₃) δ 7.29–7.11 (m, 12H), 6.93 (t, *J* = 7.4 Hz, 2H), 6.68 (d, *J* = 7.7 Hz, 4H), 4.80 (d, *J* = 15.8 Hz, 2H), 4.69 (d, *J* = 15.7 Hz, 2H), 4.46 (t, *J* = 5.6 Hz, 2H), 4.24 (m, 6H), 4.08 (m, 2H), 3.28 (s, 12H), 3.22 (brd, 2H), 2.83 (d, *J* = 5.6 Hz, 4H); ¹³C NMR (67.8 MHz, CDCl₃) δ 157.8, 137.9, 137.5, 129.6, 128.9 (2C), 128.8, 126.2, 121.6, 114.6, 105.2, 75.3, 66.7, 53.5, 53.4, 39.5. Anal. (C₄₀H₅₀N₂O₁₀S) C, H, N.

(3R,4S,5S,6R)-2,7-Bis[4-(hydroxymethyl)phenyl]methyl-3,6-bis(phenoxymethyl)-4,5-dihydroxy-1,2,7-thiadiazepine 1,1-Dioxide (7). To a solution of **12** (105.8 mg, 0.122 mmol) in ether (10 mL) was added LiBH₄ (16 mg, 0.733 mmol) followed by the addition of toluene (5 mL) and the reaction was refluxed for 2 h at 80 °C. The reaction was quenched with water (10 mL) and the water phase was extracted with 2 × 10 mL of ether. The solvent was removed, the crude product was dissolved in methanol (5 mL), and saturated HCl in ether (10 mL) was added. This was stirred overnight at room temperature. The solvent was removed and purification by flash column chromatography on silica (CH₂Cl₂/CH₃OH, 100:1–25:1) gave compound **7** (33.2 mg, 83%): IR (KBr) ν 3600–3200, 2927, 1598, 1496 cm⁻¹; [α]_D = +14.4° (*c* = 0.52, CHCl₃, 22 °C); ¹H NMR (270.2 MHz, CDCl₃) δ 7.48 (d, *J* = 8.2 Hz, 4H), 7.29 (d, *J* = 8.2 Hz, 4H), 7.24 (dd, *J* = 8.7, 7.4 Hz, 4H), 6.91 (t, *J* = 7.4 Hz, 2H), 6.81 (d, *J* = 8.7 Hz, 4H), 4.96 (m, 4H), 4.92 (brs, 2H), 4.58 (d, *J* = 5.6 Hz, 4H), 4.43 (t, *J* = 6.8 Hz, 2H), 4.32–4.10 (m, 8H); ¹³C NMR (100.2 MHz, CDCl₃) δ 159.3, 142.0, 139.5, 130.3, 128.0, 127.4, 121.8, 115.4, 74.8, 67.1, 64.5, 56.0, 52.7. Anal. (C₃₄H₃₈N₂O₈S) C, H, N.

(3R,4S,5S,6R)-2,7-Bis[4-(methoxycarbonyl)phenyl]methyl-3,6-bis(phenoxymethyl)-4,5-dihydroxy-1,2,7-thiadiazepine 1,1-Dioxide (8). To a solution of compound **12** in methanol (2.5 mL) was added HCl in ether (5 mL). The reaction mixture was stirred overnight and concentrated in vacuo. Purification by flash column chromatography on silica (CH₂Cl₂/CH₃OH, 200:1) gave the product as a colorless oil (9.8 mg, 83%): IR (CHCl₃) ν 1717, 1599, 1496, 1436 cm⁻¹; [α]_D = +6.6° (*c* = 0.98, CHCl₃, 22 °C); ¹H NMR (270.2 MHz, CDCl₃) δ 7.94 (d, *J* = 8.4 Hz, 4H), 7.46 (d, *J* = 8.4 Hz, 4H), 7.20 (dd, *J* = 8.5, 7.4 Hz, 4H), 6.93 (t, *J* = 7.4 Hz, 2H), 6.66 (d, *J* = 8.7 Hz, 4H), 4.86 (m, 4H), 4.34–4.16 (m, 6H), 4.08 (dd, *J* = 9.4, 5.4 Hz, 2H), 3.88 (s, 6H), 3.08 (s, 2H); ¹³C NMR (67.8 MHz,

CDCl₃) δ 166.9, 157.5, 143.4, 130.1, 129.7, 129.6, 127.6, 121.9, 114.5, 73.3, 67.1, 55.9, 53.2, 52.3. Anal. (C₃₆H₃₈N₂O₁₀S) C, H, N.

(3R,4S,5S,6R)-2,7-Bis[(3-iodophenyl)methyl]-4,5-bis[(2-methoxyethoxy)methoxy]-3,6-bis(phenoxymethyl)-1,2,7-thiadiazepine 1,1-dioxide (11). To a solution of **10**²⁰ (50 mg, 0.088 mmol) in DMF (2 mL) were added NaH (80% suspension, 10.5 mg, 0.35 mmol) and 3-iodobenzyl bromide (104.2, 0.35 mmol). The reaction mixture was stirred under a N₂ atmosphere overnight and concentrated in vacuo. Purification by flash column chromatography on silica gel (CH₂Cl₂/CH₃OH, 100:1) gave the product as a colorless oil (77 mg, 88%): IR (film) ν 1674, 1599, 1566 cm⁻¹; [α]_D = +14.1° (*c* = 0.81, CHCl₃, 21 °C); ¹H NMR (270 MHz, CDCl₃) δ 7.73 (s, 2H), 7.51 (appt, 4H), 7.23 (m, 4H), 7.02 (t, *J* = 7.7 Hz, 2H), 6.93 (t, *J* = 7.3 Hz, 2H), 6.70 (d, *J* = 8.9 Hz, 4H), 4.92 (d, *J* = 17.2 Hz, 2H), 4.84 (d, *J* = 7.1 Hz, 2H), 4.79 (d, *J* = 6.8 Hz, 2H), 4.76 (d, *J* = 17.4 Hz, 2H), 4.43 (t, *J* = 6.9 Hz, 2H), 4.21 (s, 2H), 4.00 (m, 4H), 3.74 (ddd, *J* = 11.0, 5.4, 4.1 Hz, 2H), 3.64 (ddd, *J* = 10.9, 4.9, 4.1 Hz, 2H), 3.42 (m, 4H), 3.27 (s, 6H); ¹³C NMR (67.8 MHz, CDCl₃) δ 157.8, 142.0, 136.3, 136.0, 130.5, 129.7, 126.5, 121.5, 114.5, 96.3, 94.5, 77.3, 71.6, 68.2, 66.1, 59.1, 53.5, 51.2. Anal. (C₄₀H₄₈I₂N₂O₁₀S) C, H, N.

(3R,4S,5S,6R)-2,7-Bis[[4-(methoxycarbonyl)phenyl]methyl]-4,5-bis[(2-methoxyethoxy)methoxy]-3,6-bis(phenoxymethyl)-1,2,7-thiadiazepine 1,1-Dioxide (12). To a solution of **10** (50 mg, 0.088 mmol) in DMF (2 mL) were added NaH (80% suspension, 10.5 mg, 0.35 mmol) and methyl 4-bromomethylbenzoate (80 mg, 0.35 mmol). The reaction mixture was stirred under a N₂ atmosphere overnight and concentrated in vacuo. Purification by flash column chromatography on silica gel (CH₂Cl₂/CH₃OH, 100:1) gave the product as a colorless oil (61 mg, 80%): IR (film) ν 1716, 1600, 1496, 1436 cm⁻¹; [α]_D = -1.0° (*c* = 1.05, CHCl₃, 21 °C); ¹H NMR (270.2 MHz, CDCl₃) δ 7.97 (d, *J* = 8.6 Hz, 4H), 7.52 (d, *J* = 8.6 Hz, 4H), 7.20 (dd, *J* = 7.7, 7.3 Hz, 4H), 6.91 (t, *J* = 7.3 Hz, 2H), 6.67 (d, *J* = 7.6 Hz, 4H), 5.00 (d, *J* = 18 Hz, 2H), 4.90 (d, *J* = 17.5 Hz, 2H), 4.85 (d, *J* = 6.8 Hz, 2H), 4.81 (d, *J* = 7.1 Hz, 2H), 4.47 (t, *J* = 6.9 Hz, 2H), 4.25 (apps, 2H), 4.02 (d, *J* = 7.1 Hz, 4H), 3.88 (s, 6H), 3.68 (m, 4H), 3.40 (m, 4H), 3.25 (s, 6H); ¹³C NMR (67.8 MHz, CDCl₃) δ 167.0, 157.8, 144.9, 130.0, 129.7, 129.0, 126.9, 121.6, 114.4, 96.2, 77.2, 71.6, 68.2, 66.0, 59.1, 53.5, 52.2, 51.9. Anal. (C₄₄H₅₄N₂O₁₄S) C, H, N.

Modeling. Symmetric versus Nonsymmetric Conformation of 2. A model for the urea-like conformation of a cyclic sulfamide was obtained by fitting **2** to the X-ray coordinates of the inhibitor of the HIV-1 protease complex of **1**. A model of the observed conformation of **2** was taken from the X-ray coordinates of the inhibitor of the HIV-1 protease complex of **2**. The above models were simplified by truncation of the P1/P1' and P2/P2' groups to methyls (see Figure 2). Relaxation of the models to the nearest local minima was accomplished with MacroModel 5.5³⁷ using the MMFF³⁸ force field. Ab initio optimizations at the B3LYP/6-31G* level with Gaussian94³⁹ were performed to further refine the geometries. The energy difference between the resulting structures was used to estimate the accessibility of the urea-like ring conformation as compared to the nonsymmetrical "flipped" conformation.

Modeling of the Ketoxime 4. Acetophenone oxime was used as a model of the ketoxime function of **4**. The model was relaxed in vacuo with MacroModel 5.5 using the MMFF force field. The model was then subjected to a 1000-step Monte Carlo run allowing rotation of the phenyl group and the C=N double bond. Two minima were identified: the *E* and *Z* isomers. Ab initio optimizations at the B3LYP/6-31G* level with Gaussian94 were performed to further refine the geometries.

Modeling of 3–8. The symmetric and nonsymmetric models of **2** were augmented with the R₁ and R₂ groups shown in Table 1 to produce the starting models for the urea-like and nonsymmetrical conformations of **3** and **5–8**. The models were further refined in MacroModel 5.5 by substructure minimization of the P2/P2' groups under the AMBER⁴⁰ force field (5.5 Å shell from the P2/P2' atoms of the enzyme portion of the HIV-1 protease complex of **2**). Since we were unable to predict

Table 2. Data Processing Statistics

	HIV-1 PR/4	HIV-1 PR/9
space group	$P2_12_12$	$P2_12_12$
wavelength (Å)	0.958	0.920
no. of crystals	5	2
cell dimensions a , b , c (Å)	58.85, 86.68, 46.97	59.55, 87.68, 47.29
d_{\min} (Å)	1.80	1.92
no. of observations	40892	28401
no. of unique reflections	18434	15933
completeness (%)	80.6	81.4
R_{merge} (%) ^a	12.4	5.5
reflections $I > 3\sigma$ (%)	52.9	60.0
reflections $I > 3\sigma$ (%) in highest resolution shell	17.0	32.0
B in resolution (Å)	1.86–1.80	1.99–1.92

^a $R_{\text{merge}} = \sum |I_i - \langle I \rangle| / \sum I_i$, where I_i is an observation of the intensity of an individual reflection and $\langle I \rangle$ is the average intensity over symmetry equivalents.

Table 3. Refinement Statistics of Final Models

	HIV-1 PR/4	HIV-1 PR/9
resolution of data (Å)	24.0–1.80	8.0–1.92
R_{cryst} (%)	21.2	19.8
R_{free} (%)	23.6	25.4
no. of atoms	1667	1628
no. of water molecules	96	78
mean B factor, protein (Å ²)	23.3	27.4
mean B factor, inhibitor (Å ²)	17.4	13.9
deviation from ideality		
bond lengths (Å)	0.007	0.011
bond angles (deg)	1.261	1.729
dihedrals (deg)	25.420	25.453
impropers (deg)	0.801	1.390

the position of the structural waters for the models of **3–8**, we instead used a GB/SA⁴¹ solvation model. Short Monte Carlo runs exploring 4–6 rotatable bonds were performed on each model under the same conditions to find reasonable positioning of the P2/P2' groups.

Crystallography. HIV-1 protease was expressed in *E. coli*.⁴² The enzyme was isolated from inclusion bodies through a slightly modified version of the method by Taylor et al.⁴³ Briefly, the inclusion body fraction was dissolved in 8 M urea, separated on a Poros Q column (Roche), refolded by dialysis at 4 °C, and finally purified on a Poros S column. The material was concentrated by ammonium sulfate precipitation, desalted, and finally concentrated on Centricon membrane centrifugation tubes (Amicon).

Crystallization was performed by the vapor diffusion method. Inhibitor (40 mM, dissolved in DMSO) was added to a 2 mg/mL protease solution giving a final molar ratio of 2:1 and incubated for 30 min on ice. Drops consisting of 5 μ L of the protease–inhibitor mixture plus 5 μ L of the crystallization buffer (50 mM MES, pH 5.5, 0.4 M NaCl, and 0.02% (w/v) NaN₃) were equilibrated against the same buffer at 4 °C. Crystals grew to a size of 0.27 mm \times 0.12 mm \times 0.10 mm within 2 weeks.

X-ray data were recorded at 4 °C on MAR imaging plates on the synchrotron beam lines I711 at MAX-lab Lund, Sweden (compound **4**), and 9.5 DRAL Daresbury, England (compound **9**). The programs DENZO and SCALEPACK were used for processing and scaling.^{44,45} A summary of data collection statistics is given in Table 2. The protease model coordinates from 1AJV were used for molecular replacement calculations.

Refinement was performed using the program packages X-PLOR (complex **9**) and CNS (complex **4**).^{46,47} The difference Fourier map ($F_o - F_c$) clearly showed the position and orientation of the inhibitor together with the positions of a large number of water molecules. The inhibitor was built manually into the electron density using the program O.⁴⁸ Water molecules were added to the structure of HIV-1 protease/**4** determined from the difference Fourier maps at chemically acceptable sites. Only solvent molecules with B values less

than 50 Å² were accepted. The R_{cryst} and R_{free} factors were used to monitor the refinement.⁴⁹ The refinement statistics are shown in Table 3.

Acknowledgment. We thank the Swedish Foundation for Strategic Research (SSF), the Swedish Medicinal Research Council (MFR), and Medivir AB for financial support.

References

- (1) Kohl, N. E.; Emini, E. A.; Schleif, W. A.; Davis, L. J.; Heimbach, J. C.; Dixon, R. A. F.; Scolnick, E. M.; Sigal, I. S. Active Human Immunodeficiency Virus Protease Is Required for Viral Infectivity. *Proc. Natl. Acad. Sci. U.S.A.* **1988**, *85*, 4686–4690.
- (2) Wei, X.; Ghosh, S. K.; Taylor, M. E.; Johnson, V. A.; Emini, E. A.; Deutsch, P.; Lifson, J. D.; Bonhoeffer, S.; Nowak, M. A.; Hahn, B. H.; Saag, M. S.; Shaw, G. M. Viral Dynamics in Human Immunodeficiency Virus Type 1 Infection. *Nature* **1995**, *273*, 117–122.
- (3) Ho, D. D.; Neumann, A. U.; Perelson, A. S.; Chen, W.; Leonard, J. M.; Markowitz, M. Rapid Turnover of Plasma Virions and CD4 Lymphocytes in HIV-1 Infection. *Nature* **1995**, *373*, 123–126.
- (4) Patick, A. K.; Mo, H.; Markowitz, M.; Appelt, K.; Wu, B.; Musick, L.; Kalish, V.; Kaldor, S.; Reich, S.; Ho, D.; Webber, S. Antiviral and Resistance Studies of AG1343, an Orally Bioavailable Inhibitor of Human Immunodeficiency Virus Protease. *Antimicrob. Agents Chemother.* **1996**, *40*, 292–297.
- (5) Palella, F. J., Jr.; Delaney, K. M.; Moorman, A. C.; Loveless, M. O.; Fuhrer, J. S. G. A.; Aschman, D. J.; Holmberg, S. D. Declining Morbidity and Mortality Among Patients with Advanced Human Immunodeficiency Virus Infection. *N. Engl. J. Med.* **1998**, *338*, 853–860.
- (6) Ala, P. J.; Huston, E. E.; Klabe, R. M.; McCabe, D. D.; Duke, J. L.; Rizzo, C. J.; Korant, B. D.; DeLoskey, R. J.; Lam, P. Y. S.; Hodge, N.; Chang, C.-H. Molecular Basis of HIV-1 Protease Drug Resistance: Structural Analysis of Mutant Protease Complexed with Cyclic Urea Inhibitors. *Biochemistry* **1997**, *36*, 1573–1580.
- (7) Mellors, J. W.; Larder, B. A.; Schinazi, R. F. Mutations in HIV-1 Reverse Transcriptase and Protease Associated with Drug Resistance. *Int. Antivir. News* **1995**, *3*, 8–13.
- (8) Erickson, J. W. The Not-So-Great Escape. *Nature Struct. Biol.* **1995**, *2*, 523–529.
- (9) Tisdale, M. HIV Protease Inhibitors-Resistance Issues. *Int. Antivir. News* **1996**, *4*, 41–43.
- (10) Appelt, K. Crystal Structures of HIV-1 Protease-Inhibitor Complexes. *Perspect. Drug Discovery Des.* **1993**, *1*, 23–48.
- (11) Jadhav, P. K.; Woerner, F. J.; Lam, P. Y. S.; Hodge, C. N.; Eyermann, C. J.; Man, H.-W.; Danek, W. F.; Bacheler, L. T.; Rayner, M. M.; Meek, J. L.; Erickson-Viitanen, S.; Jackson, D. A.; Calabrese, J. C.; Schadt, M.; Chang, C.-H. Nonpeptide Cyclic Cyanoguanidines as HIV-1 Protease Inhibitors: Synthesis, Structure–Activity Relationships and Crystal Structure Studies. *J. Med. Chem.* **1998**, *41*, 1446–1455.
- (12) Turner, S. R.; Strohbach, J. W.; Tommasi, R. A.; Aristoff, P. A.; Johnson, P. D.; Skulnich, H. I.; Dolak, L. A.; Seest, E. P.; Tomich, P. K.; Bohanon, M. J.; Horng, M.-M.; Lynn, J. C.; Chong, K.-T.; Hinshaw, R. R.; Watenpaugh, K. D.; Janakiraman, M. N.; Thaisrivongs, S. Tipranavir (PNU 140960): A potent, Orally Bioavailable nonpeptide HIV Protease Inhibitor of the 5,6-Dihydro-4-hydroxy-2-pyrone Sulfonamide Class. *J. Med. Chem.* **1998**, *41*, 3467–3476.
- (13) Wlodawer, A.; Erickson, J. W. Structure-Based Inhibitors of HIV-1 Protease. *Annu. Rev. Biochem.* **1993**, *62*, 543–585.
- (14) Wang, Y.-X.; Freedberg, D. I.; Wingfield, P. T.; Stahl, S. J.; Kaufman, J. D.; Kiso, Y.; Bhat, T. N.; Erickson, J. W.; Torchia, D. A. Bound Water Molecules at the Interface Between the HIV-1 Protease and a Potent Inhibitor, KNI-272, Determined by NMR. *J. Am. Chem. Soc.* **1996**, *118*, 12287–12290.
- (15) Wang, Y.-X.; Freedberg, D. I.; Grzesik, S.; Torchia, D. A.; Wingfield, P. T.; Kaufman, J. D.; Stahl, S. J.; Chang, C.-H.; Hodge, C. N. Mapping hydration Water Molecules in the HIV-1 Protease/DMP 323 Complex in Solution By NMR Spectroscopy. *Biochemistry* **1996**, *35*, 12694–12704.
- (16) Yamazaki, T.; Hinck, A. P.; Wang, Y.-X.; Nicholson, L. K.; Torchia, D. A.; Wingfield, P. S.; S. J.; Kaufman, J. D.; Chang, C.-H.; Domaille, P. J.; Lam, P. Y. S. Three-Dimensional Solution Structure of the HIV-1 Protease Complexed with DMP323, a Novel Cyclic Urea-Type Inhibitor, Determined by Nuclear Magnetic Resonance Spectroscopy. *Protein Sci.* **1996**, *5*, 495–506.
- (17) Grzesiek, S.; Bax, A.; Nicholson, L. K.; Yamazaki, T.; Wingfield, P.; Stahl, S. J.; Eyermann, C. J.; Torchia, D. A.; Hodge, C. H.; Lam, P. Y. S.; Jadhav, P. K.; Chang, C.-H. NMR Evidence for the Displacement of a Conserved Interior Water Molecule in HIV Protease by a Non-Peptide Cyclic Urea-Based Inhibitor. *J. Am. Chem. Soc.* **1994**, *116*, 1581–1582.

- (18) Ishima, R.; Wingfield, P. T.; Stahl, S. J.; Kaufman, J. D.; Torchia, D. A. Using Amide 1H and 15N Transverse relaxation To Detect Millisecond Time-Scale Motions in Predeuterated Proteins: Applications to HIV-1 Protease. *J. Am. Chem. Soc.* **1998**, *120*, 10534–10542.
- (19) Lam, P. Y. S.; Jadhav, P. K.; Eyermann, C. J.; Hodge, C. N.; Ru, Y.; Bacheler, L. T.; Meek, J. L.; Otto, M. J.; Rayner, M. M.; Wong, Y. N.; Chang, C.-H.; Weber, P. C.; Jackson, D. A.; Sharpe, T. R.; Erickson-Viitanen, S. Rational Design of Potent, Bioavailable, Nonpeptide Cyclic Ureas as HIV Protease Inhibitors. *Science* **1994**, *263*, 380–384.
- (20) Hultén, J.; Bonham, N. M.; Nillroth, U.; Hansson, T.; Zuccarello, G.; Bouzide, A.; Åqvist, J.; Classon, B.; Danielson, H. U.; Karlén, A.; Kvarnström, I.; Samuelson, B.; Hallberg, A. Cyclic HIV-1 Protease Inhibitors Derived from Mannitol: Synthesis, Inhibitory Potencies, and Computational Predictions of Binding Affinities. *J. Med. Chem.* **1997**, *40*, 885–897.
- (21) Bäckbro, K.; Löwgren, S.; Österlund, K.; Atepo, J.; Unge, T.; Hultén, J.; Bonham, N. M.; Schaal, W.; Karlén, A.; Hallberg, A. Unexpected Binding Mode of a Cyclic Sulfamide HIV-1 Protease Inhibitor. *J. Med. Chem.* **1997**, *40*, 898–902.
- (22) Hallberg, A.; Westfelt, L.; Holm, B. Palladium-Catalyzed Arylation of Methyl Vinyl Ether. *J. Org. Chem.* **1981**, *46*, 5414–5415.
- (23) Cabri, W.; Candiani, I.; Bedeschi, A.; Santi, R. Ligand-Controlled α -Regioselectivity in Palladium-Catalyzed Arylation of Butyl Vinyl Ether. *J. Org. Chem.* **1990**, *55*, 3654–3655.
- (24) Larhed, M.; Hallberg, A. Direct Synthesis of Cyclic Ketals of Acetophenones by Palladium-Catalyzed Arylation of Hydroxyalkyl Vinyl Ethers. *J. Org. Chem.* **1997**, *62*, 7858–7862.
- (25) Harada, T.; Ohno, T.; Kobayashi, S.; Mukaiyama, T. The Catalytic Friedel–Crafts Acylation Reaction and the Catalytic Beckmann Rearrangement Promoted by a Gallium(III) or a Antimony(V) Cationic Species. *Synthesis* **1991**, 1216–1220.
- (26) Andersson, C.-M.; Larsson, J.; Hallberg, A. *J. Org. Chem.* **1990**, *55*, 5757.
- (27) Brown, H. S.; Narasimhan, S.; Choi, Y. M. Selective Reductions. 30. Effect on Cation and Solvent on the Reactivity of Saline Borohydrides for Reduction of Carboxylic Esters. Improved Procedures for the Conversion of Esters to Alcohols by Metal Borohydrides. *J. Org. Chem.* **1982**, *47*, 4702–4708.
- (28) Danielson, U. H.; Lindgren, M. T.; Markgren, P. O.; Nillroth, U. Investigation of an Allosteric Site of HIV-1 Proteinase Involved in Inhibition by Cu²⁺. *Adv. Exp. Med. Biol.* **1998**, *463*, 99–103.
- (29) Nillroth, U.; Vrang, L.; Markegren, P.-O.; Hultén, J.; Hallberg, A.; Danielson, U. H. Human Immunodeficiency Virus Type 1 Proteinase Resistance to Symmetric Cyclic Urea Inhibitor Analogues. *Antimicrob. Agents Chemother.* **1997**, *41*, 2383–2388.
- (30) Abola, E. E.; Sussman, J. L.; Prilusky, J.; Manning, N. O. Protein Data Bank Archives of Three-Dimensional Macromolecular Structures. In *Methods in Enzymology*; Carter, Jr., C. W., Sweet, R. M., Eds.; Academic Press: San Diego, 1997; Vol. 277, pp 556–571.
- (31) Sussman, J. L.; Lin, D. J.; Manning, N. O.; Prilusky, J.; Ritter, O.; Abola, E. E. Protein Data Bank (PDB): Database of Three-Dimensional Structural Information of Biological Macromolecules. *Acta Crystallogr.* **1998**, *D54*, 1078–1084.
- (32) Lam, P. Y. S.; Ru, Y.; Jadhav, P. K.; Aldrich, P. E.; DeLuca, G. V.; Eyermann, C. J.; Chang, C.-H.; Emmet, G.; Holler, E. R.; Daneker, W. F.; Li, L.; Confalone, P. N.; McHugh, R. J.; Han, Q.; Li, R.; Markwalder, J. A.; Seitz, S. P.; Sharpe, T. R.; Bacheler, L. T.; Rayner, M. M.; Klabe, R. M.; Shum, L.; Winslow, D. L.; Kornhauser, D. M.; Jackson, D. A.; Erikson-Viitanen, S.; Hodge, C. N. Cyclic HIV Protease Inhibitors: Synthesis, Conformational Analysis, P2/P2' Structure–Activity Relationship, and Molecular Recognition of Cyclic Ureas. *J. Med. Chem.* **1996**, *39*, 3514–3525.
- (33) Allen, F. H.; Kennard, O. 3D Search and Research Using the Cambridge Structural Database. *Chem. Des. Autom. News* **1993**, *8*, 1 and 31–37.
- (34) Energy calculations were conducted to test the hypothesis of a more stable *E* isomer. Under the MMFF empirical force field of MacroModel, the *E* isomer was calculated to be 3.4 kcal/mol more stable than the *Z* isomer. Since oximes are not well parametrized with the above force field, an ab initio calculation was performed. At the B3LYP/6-31G* level of theory, the *E* isomer was calculated to be 2.6 kcal/mol more stable than the *Z* isomer. Assuming that the reaction was not overwhelmingly kinetically controlled, we used the *E* isomer in our models.
- (35) Han, Q.; Chang, C.-H.; Li, R.; Ru, Y.; Jadhav, P. K.; Lam, P. Y. S. Cyclic HIV Protease Inhibitors: Design and Synthesis of Orally Bioavailable, Pyrazole P2/P2' Cyclic Ureas with Improved Potency. *J. Med. Chem.* **1998**, *41*, 2019–2028.
- (36) For a discussion on the displacement of corresponding structural water molecules in other systems, see: Melnick, M.; Reich, S. H.; Lewis, K. K.; Mitchell, L. J., Jr.; Nguyen, D.; Trippie, A. J.; Dawson, H.; Davies, J. F., II; Appelt, K.; Wu, B.-W.; Musick, L.; Gehlaar, D. K.; Webber, S.; Shetty, B.; Kosa, M.; Kahil, D.; Andrada, D. Bis Tertiary Amide Inhibitors of the HIV-1 Protease Generated via Protein Structure-Based Iterative Design. *J. Med. Chem.* **1996**, *39*, 2795–2811.
- (37) Mohamadi, F.; Richards, N. G. J.; Guida, W. C.; Liskamp, R.; Lipton, M.; Caufield, C.; Chang, G.; Hendrickson, T.; Still, W. C. MacroModel—An Integrated Software System for Modeling Organic and Bioorganic Molecules Using Molecular Mechanics. *J. Comput. Chem.* **1990**, *11*, 440–467.
- (38) Halgren, T. A. Merck Molecular Force Field. 1. Basis, Form, Scope, Parametrization, and Performance of MMFF94. *J. Comput. Chem.* **1996**, *17*, 490–519.
- (39) Frisch, M. J.; Trucks, G. W.; Schlegel, H. B.; Gill, P. M. W.; Johnson, B. G.; Robb, M. A.; Cheeseman, J. R.; Keith, T.; Petersson, G. A.; Montgomery, J. A.; Raghavachari, K.; Al-Laham, M. A.; Zakrzewski, V. G.; Ortiz, J. V.; Foresman, J. B.; Cioslowski, J.; Stefanov, B. B.; Nanayakkara, A.; Challacombe, M.; Peng, C. Y.; Ayala, P. Y.; Chen, W.; Wong, M. W.; Andres, J. L.; Replogle, E. S.; Gomperts, R.; Martin, R. L.; Fox, D. J.; Binkley, J. S.; Defrees, D. J.; Baker, J.; Stewart, J. P.; Head-Gordon, M.; Gonzalez, C.; Pople, J. A. *Gaussian 94, Revision D. 4*; Gaussian, Inc.: Pittsburgh, PA, 1995.
- (40) McDonald, D. Q.; Still, W. C. AMBER* Torsional Parameters for the Peptide Backbone. *Tetrahedron Lett.* **1992**, *33*, 7743–7746.
- (41) Still, W. C.; Tempczyk, A.; Hawley, R. C.; Hendrickson, T. Semianalytical Treatment of Solvation for Molecular Mechanics and Dynamics. *J. Am. Chem. Soc.* **1990**, *112*, 6127–6129.
- (42) Bäckbro, K.; Zhang, H.; Vrang, L.; Öberg, B.; Unge, T. Unpublished results.
- (43) Taylor, A.; Brown, D. P.; Kadam, S. M.; Kohlbrenner, W. E.; Weigl, D.; Turon, M. C.; Katz, L. High-level expression and purification of mature HIV-1 protease in *Escherichia coli* under control of the araBAD promoter. *Appl. Microbiol. Biotechnol.* **1992**, *205*–210.
- (44) Gewirth, D.; Otwinovski, Z. The SCALEPACK Manual.
- (45) Otwinovski, Z.; Minor, W. The HKL Program Suite.
- (46) Brunger, A. T.; Adams, P. D.; Clore, G. M.; Delano, W. L.; Gros, P.; Grosse-Kunstleve, R. W.; Jiang, J.-S.; Kuszewski, J.; Nilges, M.; Pannu, N. S.; Read, R. J.; Rice, L. M.; Simonson, T.; Warren, G. L. Crystallography & NMR System: A New Software Suite for Macromolecular Structure Determination. *Acta Crystallogr.* **1998**, *D54*, 905–921.
- (47) Brünger, A. T.; Kuriyan, J.; Karplus, M. Crystallographic R factor refinement by molecular dynamics. *Science* **1987**, *235*, 458–460.
- (48) Jones, T. A.; Zou, J.-Y.; Cowan, S. W.; Kjeldgaard, M. Improved methods for building protein models in electron density maps and the location of errors in these models. *Acta Crystallogr.* **1991**, *A47*, 110–119.
- (49) $R_{\text{cryst}} = \frac{\sum ||F_o| - |F_c||}{\sum |F_o|}$, where F_o and F_c are the observed and calculated structure factor amplitudes, respectively. R_{free} is equivalent to R_{crystal} but calculated for a randomly chosen set of reflections that were omitted from the refinement process.
- (50) Kraulis, P. J. MOLSCRIPT: a program to produce both detailed and schematic plots of protein structures. *J. Appl. Crystallogr.* **1991**, *24*, 946–950.

JM991054Q